

LATEST RESULTS OF CW 100 mA ELECTRON RF GUN FOR NOVOSIBIRSK ERL BASED FEL *

V. N. Volkov †, V. Arbuzov, E. Kenzhebulatov, E. Kolobanov, A. Kondakov, E. Kozyrev, S. Krutikhin, I. Kuptsov, G. Kurkin, S. Motygin, A. Murasev, V. Ovchar, V.M. Petrov, A. Pilan, V. Repkov, M. Scheglov, I. Sedlyarov, S. Serednyakov, O. Shevchenko, S. Tararyshkin, A. Tribendis, N. Vinokurov, BINP SB RAS, Novosibirsk, Russia

Abstract

Continuous wave (CW) 100 mA electron rf gun for injecting the high-quality 300-400 keV electron beam in Novosibirsk Energy Recovery Linac (ERL) and driving Free Electron Laser (FEL) was developed, built, and commissioned at BINP SB RAS. The RF gun consists of normal conducting 90 MHz rf cavity with a gridded thermionic cathode unit. Bench tests of rf gun is confirmed good results in strict accordance with our numerical calculations. The gun was tested up to the design specifications at a test bench that includes a diagnostics beam line. The rf gun stand testing showed reliable work, unpretentious for vacuum conditions and stable in long-term operation. The design features of different components of the rf gun are presented. Preparation and commissioning experience is discussed. The latest beam results are reported.

INTRODUCTION

Recent projects of advanced sources of electromagnetic radiation [1] are based on the new class of electron accelerators where the beam current is not limited by the power of rf system – energy recovery linacs (ERLs). Such accelerators require electron guns operating in continuous wave (cw) mode with high average current. The only solution is an rf gun, where the cathode is installed inside the rf cavity. RF guns have no problem with degradation of the cathode due to absence of back bombardment electrons so the vacuum condition is not important there. The most power Novosibirsk FEL [2] can be more powerful by one order on magnitude with this rf gun [3-5]. Measured rf gun characteristics are presented in Table 1.

RF GUN AND DIAGNOSTIC STAND

The rf gun and diagnostic stand are presented in Fig. 1.

The RF gun cavity is made on the base of standard bimetallic cavity of Novosibirsk ERL Detailed information can be found in [3-5]. Only the insert with the thermionic cathode-grid unit is built into the cavity. The gridded thermionic dispenser cathode is driven by special modulator with GaN rf transistor. The insert focusing electrode executes the strong rf focusing of the beam just near the cathode that ensures the beam emittance compensation at the relatively low electric field at the cathode. Also it ensures the absolute absence of dark currents in the beam.

There are in the stand: 30 kW water cooled beam dump

* Work supported by Russian Science Foundation (project N 14-50-00080)

† v.n.volkov@inp.nsk.su

with 5 cm lead radiation shield, wideband Wall Current Monitor (WCM2) inserted into the replaceable target, Transition Radiation Sensor, the pair of standard WCM, three focusing solenoids, and the testing cavity.

Table 1: Measured RF Gun Characteristics

Average beam current, mA	≤100
Cavity Frequency, MHz	90
Bunch energy, keV	100 ÷ 400
Bunch duration (FWHM), ns	0.06 ÷ 0.6
Bunch emittance, mm mrad	10
Bunch charge, nC	0.3 ÷ 1.12
Repetition frequency, MHz	0.01 ÷ 90
Radiation Doze Power, mR/h	100/2m
Operating pressure, Torr	10 ⁻⁹ ...10 ⁻⁷
Cavity RF loses, kW	20

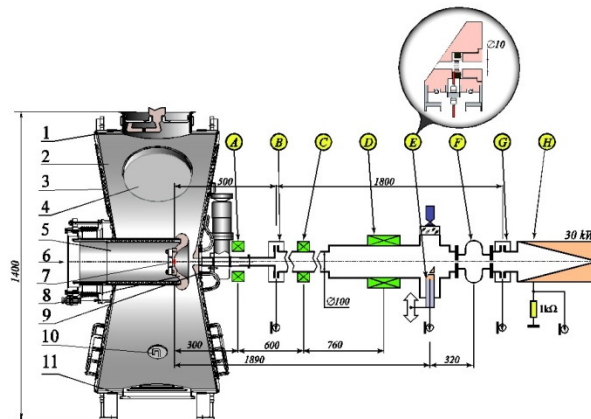


Figure 1: RF gun and stand layout: 1-Power input coupler; 2- Cavity shell; 3-Cavity back wall; 4-Sliding tuner; 5-Insert; 6-Cathode injection/extraction channel; 7-Thermionic cathode-grid unit; 8-Concave focusing electrode; 9-Cone like nose; 10-Loop coupler; 11-Vacuum pumping port; A-Emittance compensation solenoid; B-First Wall Current Monitor (WCM); C, D -Solenoids ; E-Wideband WCM and transition radiation target; F – Test Cavity; G-third WCM; H-Faraday cup and Water-cooled beam dump.

STAND TESTING RESULTS

Beam Current Regulation

There are some methods of beam current increasing: decreasing of the grid bias voltage (V_{bias}), increasing of the modulator pulse voltage (V_{puls}), and increasing of the

repetition frequency. Also there must be increased the cathode heating voltage (V_{heat}) to compensate the cathode emission ability derating. The applying of these methods is shown in Fig 2.

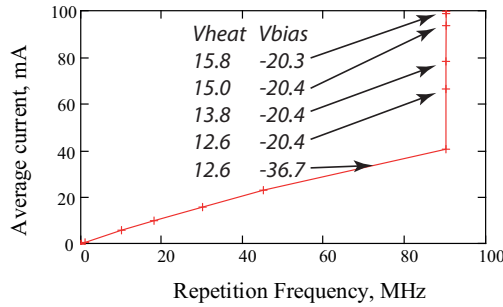


Figure 2: Typical method of current rising.

Calibration of Cavity Voltage Meter

To measure the beam energy there is used the measuring of time delay between two wall current monitors. Since the particle velocities at the relatively low energy are lower than speed of light. It is demonstrated in Fig. 3. This effect was used for the calibration of the cavity voltage meter. The calibration has a high accuracy.

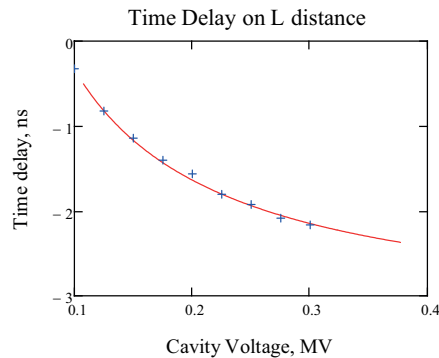


Figure 3: Measured data fitting by theory curve.

Cavity Testing up to 400 kV

The cavity voltage was increased with step by step method. After each step there required 1/2 an hour to normalize the vacuum condition (see Fig. 4).

Maximum beam current at 400 kV was limited by the beam dump permissible power.

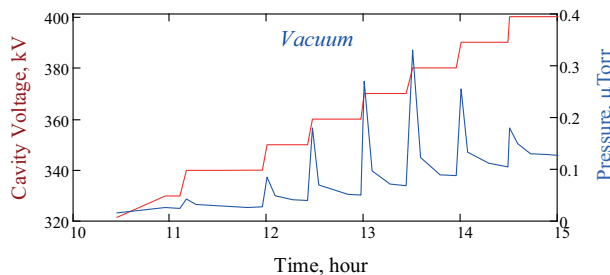


Figure 4: Cavity testing process behavior.

Launch Phase Functions

Energy distribution along the bunch is changed if the launch phase will be changed. The energy of head particles becomes lower at lower launch phases. It is used for velocity bunching at a drift space and the phase instability (jitter) compensation. Also there is changed the bunch energy as it shown in Fig. 5. The maximal bunch particle energy is at 68° , and minimal bunch length at 31° .

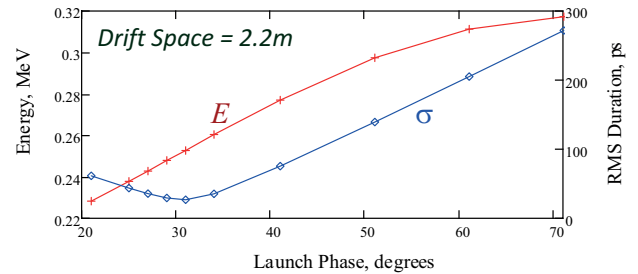


Figure 5: Launch phase functions.

Particle Distribution along the Bunch

There are complex particle distributions along the bunch due to plasma oscillation into a cathode-grid unit. On the drift space this distribution are changed significantly. The example of this at the launch phase of 31° is shown in Fig. 6. Frontal spike is formed into cathode-grid gap. Then it grows and becomes short of about 20 ps FWHM while traveling along the drift space.

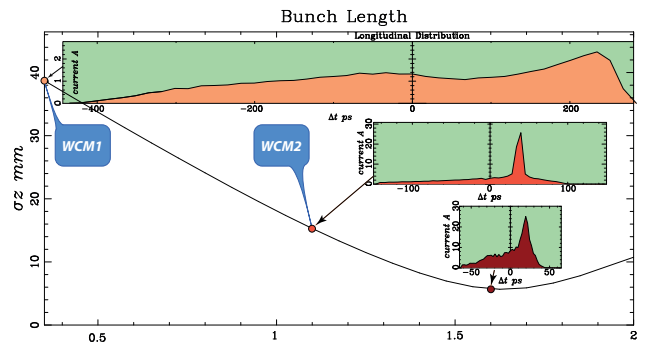


Figure 6: Bunch duration behaviour on the drift space.

Launch Phase Jitter Compensation

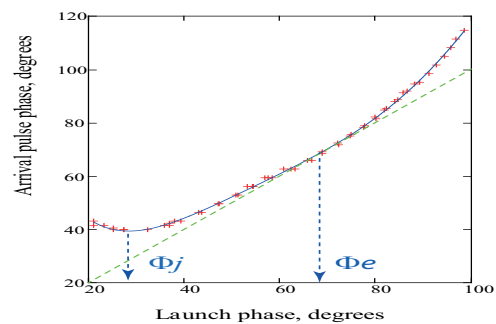


Figure 7: Arrival pulse phase behavior.

The jitter compensation effect has measured between two WCMs with 1.2 m distance between them (see Fig. 7). At the launch phase of 27 degrees the arrival time is independent on launch phase so the jitter is compen-

Content from this work may be used under the terms of the CC BY 3.0 licence (© 2018). Any distribution of this work must maintain attribution to the author(s), title of the work, publisher, and DOI.

sated there, i.e. the requirement to the phase stability of the modulator pulses is not high at the launch phase of 27°.

Cathode-Grid Plasma Oscillation Effect

Calculations and experiments have shown the plasma oscillation effect depends on the cathode emission ability. For a low emission ability the bunch at the end of the drift space becomes having two parts. The excitation of a testing cavity by such a bunch will be having anomalous valley due to interfere effect between these parts.

Numerical modeling of the excitation of the test cavity for two HOMs by such bunches is presented in the upper of Fig. 8. And the experiments are at the bottom where the emission ability was regulating by cathode heating voltage.

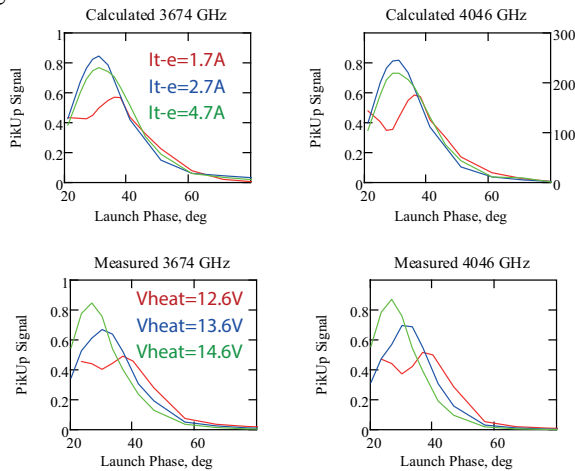


Figure 8: Excitations of test cavity HOMs. Calculations (at the top) and experiment (at the bottom) shows the interference effect for the low cathode emission ability.

Emittance Measurements

Bunch emittance was measured by solenoid focusing method when the spot size of the beam focussed to a target is measured through CCD camera registering the transition radiation.

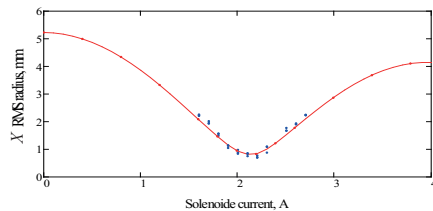


Figure 9: Measured and calculated beam behaviors.

The measured data behaviour on the focusing solenoid strength conforms to ASTRA [6] numerically calculated behaviour (see Fig. 9) with the accuracy of 9%. It corresponds to beam emittance of 15 mm mrad. The emittance can be compensated by proper focusing to 10 mm mrad.

Dark Currents

Two places in the RF gun cavity with peak surface field of 10-14 MV/m are the sources of field emitted dark cur-

rents (see Fig. 10). There are no dark currents in the beam absolutely since dark current trajectories are far from the beam.

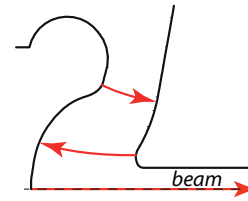


Figure 10: Dark current trajectories in the RF gun cavity.

Radiation Background

The source of bremsstrahlung radiation is the field emission current described by Fowler-Nordheim equation. Radiation background was measured behind the cavity wall with the thickness of 15 mm. The enhancement factor measured is found to be $\beta=628$. It was used as the base for calculation of enhancement factors for different thickness (10, 5, 3 mm), for bremsstrahlung power, for field emission particle power, and for field emission current (see Fig. 11). The enhancement factor for emission current is found to be $\beta_I=1250$. For the comparison, it large by one order on magnitude than the enhancement factor of superconducting cavities preparing with a perfect modern technology.

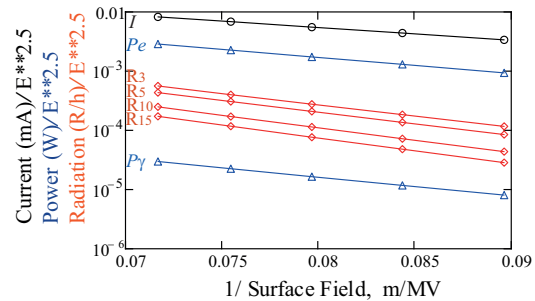


Figure 11: Calculated and measured (R15) field emission process.

REFERENCES

- [1] Vinokurov, N. A., Levichev, E. B., 2015. Undulators and wigglers for the production of radiation and other applications, *Physics-Uspekhi*. 58 850–871.
- [2] Volkov V.N., *et al.*, “First test results of RF gun for the Race-Track Microtron Recuperator of BINP SB RAS”, in *Proc. RuPAC’12*, Sep. 2012, Saint-Petersburg, Russia, paper TUPPB049.
- [3] Volkov V., *et al.*, “Thermionic cathode-grid assembly simulations for rf guns”, in *Proc. PAC’09*, Vancouver, Canada, May. 2009, paper MOYRF087.
- [4] V. Volkov, *et al.*, Thermocathode Radio-Frequency Gun for the Budker Institute of Nuclear Physics Free-Electron Laser. ISSN 1547-4771, *Physics of Particles and Nuclei Letters*, 2016, Vol. 13, No. 7, pp. 827–830.
- [5] Kulipanov, *et al.*, Novosibirsk Free Electron Laser—Facility Description and Recent Experiments, *IEEE Transactions on Terahertz Science and Technology* 5. doi:10.1109/ TTHZ. 2015. 2453121.
- [6] K. Floettmann, ASTRA User’s Manual, http://www.desy.de/~mpyflo/Astra_documentation.